

Electronic structure of a 4-Å diameter carbon nanotube placed on a patterned hydrogen-terminated Si(001):3 × 1 surface and the effect of electric field

Shyamal Konar and Bikash C. Gupta*

Department of Physics, Visva-Bharati, Santiniketan 731235, India

(Received 16 January 2011; revised manuscript received 26 April 2011; published 21 June 2011)

We have performed total-energy-minimization calculations to obtain the most stable geometry of carbon nanotube (CNT)(3,3) integrated on patterned hydrogen-terminated Si(001):3 × 1 surfaces. The electrical properties of the integrated system are studied through band-structure analysis. Charge-redistribution analysis and work-function calculations are also done. In addition, the effect of external electric field on the electrical properties of the most stable CNT(3,3) on the patterned hydrogen-terminated Si(001):3 × 1 surface is examined and it is found that depending on the magnitude of the electric field, the CNT(3,3) on the surface changes its conducting character. Therefore, this system may be used as a switching device by tuning the applied electric field.

DOI: [10.1103/PhysRevB.83.245412](https://doi.org/10.1103/PhysRevB.83.245412)

PACS number(s): 71.15.Mb, 31.15.A–, 68.43.–h

I. INTRODUCTION

After the discovery and characterization of carbon nanotubes (CNT),¹ the research interest in the field of nanotubes has grown to a great extent because of their outstanding electrical and mechanical properties.^{2–8} In fact, there are several proposals for the technological applications of CNTs as nanodevices or as wiring materials in circuit devices. However, for practical applications, the CNTs have to be integrated with a suitable substrate. The direct integration of CNTs with the well-established semiconducting substrates have added a new dimension to nanoscience research for the development of hybrid nanostructures. Though a variety of hybrid nanostructures with different structural and electrical properties may be configured by spinning, slipping, and rolling of CNTs on the substrate, only a few such configurations lead to stable hybrid structures and these stable structures may be realized in practice. Therefore, a detailed understanding of the structural and electrical properties of the CNT supported by a semiconducting substrate is of great importance.

Among the semiconducting substrates, the silicon substrate is one of the well-suited substrates for the integration of CNT. Several theoretical studies on the interaction of metallic CNTs with the Si(001) surface and their possible stable alignments on the Si(001) surface have been done recently.^{9–12} In addition, the interaction of semiconducting CNTs with the Si(001) surface has also been studied theoretically.^{13–15} However, some studies indicate that the hydrogen-terminated Si(001) surface is preferable for growing ordered nanostructures on a Si substrate. For example, the alignments and stability of CNTs on a hydrogen-terminated Si(001):2 × 1 substrate have been observed in recent experimental studies.^{15–20} Note that the hydrogen-terminated Si(001) surface reconstructs into various patterns, such as 1 × 1, 2 × 1, and 3 × 1 patterns.^{21–26} These hydrogen-terminated Si(001) surfaces may be patterned (manipulated) according to our desire by removing selected hydrogen atoms from the surface with the help of a scanning-tunneling-microscope (STM) tip.^{27,28} A number of recent theoretical studies indicate that desired wire structures may be developed on patterned (or modified) hydrogen-terminated Si(001) surfaces. We therefore consider a hydrogen-terminated Si(001) surface and pattern (or modify) it in various possible

ways for the integration of CNT on the Si(001) surface. As it is not possible to deal with all the hydrogen-terminated surfaces in a single endeavor, we therefore, consider only the patterned hydrogen-terminated Si(001):3 × 1 surface for the integration of CNT on a silicon substrate. In other words, the patterned hydrogen-terminated Si(001):3 × 1 surface is chosen as a substrate for the integration of CNT. We note that the Si(001):3 × 1 surface may be obtained experimentally by wet chemical etching and this is an attempt to understand the possible routes for integration of a CNT on a patterned hydrogen-terminated Si(001):3 × 1 surface.

Among various possible CNTs, a CNT with a 4-Å diameter is considered here for studying the interaction of CNT with a patterned hydrogen-terminated silicon substrate. The CNTs with 4-Å diameter are CNT(3,3), CNT(5,0), and CNT(4,2), respectively. The reasons behind choosing a CNT with a 4-Å diameter are that (i) these CNTs have experimentally been synthesized,²⁹ (ii) they possess different interesting physical properties, and (iii) these smaller-diameter CNTs have larger curvature energy and consequently they are structurally more sensitive than the larger-diameter CNTs. Furthermore, for a better commensuration between the substrate and the CNT, the CNT(3,3) is chosen among the 4-Å diameter CNTs for studying the integration of CNT on the patterned hydrogen-terminated Si(001):3 × 1 surface. The goal of this study is to understand the energetics, the electrical and structural properties, the work function, and the Stark effect of CNT(3,3) integrated with a patterned hydrogen-terminated Si(001):3 × 1 surface.

The paper is organized as follows. The method and the parameters are given in Sec. II. The results and discussions are presented in Sec. III, and, finally, we summarize our findings in Sec. IV.

II. APPROACH AND METHOD

First-principles total-energy calculations were carried out within density-functional theory at zero temperature using the VASP code.^{30–33} The wave functions are expressed by plane waves with a cutoff energy $|k + G|^2 \leq 300$ eV. The Brillouin-zone (BZ) integrations are performed by using the

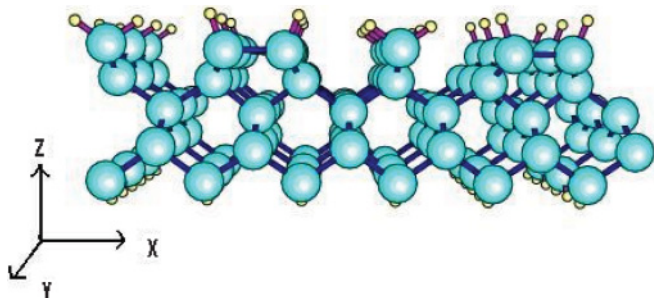


FIG. 1. (Color online) The hydrogen-terminated Si(001): 3×1 surface within the 6×3 supercell. The bigger circles correspond to the surface Si atoms while the surface hydrogen atoms are represented by the smaller circles.

Monkhorst-Pack scheme with $4 \times 4 \times 1$ k -point meshes for 3×2 primitive cells. The interaction between valence electrons and ion cores is represented by Vanderbilt-type ultrasoft pseudopotentials and results for fully relaxed atomic structures are obtained using the PW91 generalized-gradient approximation (GGA). The preconditioned-conjugate-gradient method is used for the wave-function optimization and the conjugate-gradient method for ionic relaxation. The convergence criteria for energy are taken to be 10^{-5} eV and the systems are relaxed until the forces are below 0.005 eV/Å.

The hydrogen-terminated Si(001): 3×1 surface is represented by a repeated slab geometry. As shown in Fig. 1, each slab consists of five Si atomic planes with hydrogen atoms passivating both the top- and the bottom-layer Si atoms of the slab (see Fig. 1). The top layer of the slab consists of monohydride and dihydride Si atoms that arrange themselves in such a regular fashion that the surface pattern becomes 3×1 . During calculations, the consecutive slabs are separated by a vacuum space of 22 Å to avoid any interaction with their repeating images^{34–37} when the CNT is accommodated on the slab. The lateral intertube distance along $[01\bar{1}]$ direction is kept ≈ 8 Å to avoid intertube interaction. The Si atoms constituting the top four layers of the slab are allowed to relax along with the hydrogen atoms on the top. The Si atoms of the bottom layer and the hydrogen atoms passivating the bottom-layer silicon atoms are kept fixed to simulate the bulklike termination. The convergence with respect to the number of Si layers of the slab has already been examined earlier³⁴ and it was found that five Si layers are sufficient to realize the Si(001) surface. To ensure a common periodicity of the CNT and the Si(001) surface, the Si slab is squeezed along the Y $[1\bar{1}0]$ direction by 3.25%. The expansion of the slab along X $[110]$ and Z $[001]$ directions due to the elastic property is taken into consideration.

The hydrogen-terminated Si(001): 3×1 surface is patterned in three distinct ways by removing different sets of hydrogen atoms from the surface as described below.

First, within the 3×2 supercell, one hydrogen from each Si atom of two consecutive Si rows (a dihydride-Si row and a monohydride-Si row) extended along the Y direction is removed. The surface pattern developed after the removal of such selected hydrogen atoms from the surface is identified by us as a hydrogen-terminated Si(001) surface with pattern

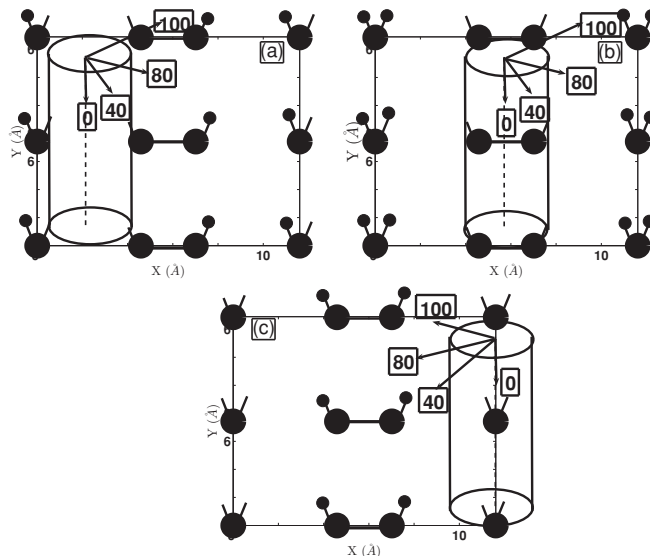


FIG. 2. Schematic diagram of the top layer of the patterned hydrogen-terminated Si(001): 3×1 surface having (a) pattern 1, (b) pattern 2, and (c) pattern 3 within a 3×2 supercell integrated with CNT(3,3) for various rotations. The 3×2 supercell is closed by thick borders. Two adjacent dangling-bond wires extending along the Y $[1\bar{1}0]$ direction are visible. The bigger circles correspond to the surface Si atoms while the surface hydrogen atoms are represented by the smaller circles.

1 and this is schematically shown in Fig. 2(a). The patterned hydrogen-terminated Si(001): 3×1 surface having pattern 1 contains 30 Si atoms and 16 hydrogen atoms within the 3×2 supercell.

Second, within the 3×2 supercell, all the hydrogen atoms attached to the Si atoms of two consecutive monohydride-silicon rows extended along the Y direction are removed and the consequent surface pattern is identified by us as the hydrogen-terminated Si(001): 3×1 surface with pattern 2. This surface pattern is schematically shown in Fig. 2(b). The patterned hydrogen-terminated Si(001): 3×1 surface having pattern 2 contains 30 silicon atoms along with 16 hydrogen atoms within the 3×2 supercell.

Third, within the 3×2 supercell, all the hydrogen atoms attached to the silicon atoms of a monomer-Si row on the surface extended along the Y direction are removed and the resultant surface pattern is identified by us as the hydrogen-terminated Si(001): 3×1 surface with pattern 3. The surface pattern is schematically shown in Fig. 2(c). The patterned hydrogen-terminated Si(001): 3×1 surface having pattern 3 contains 30 silicon atoms along with 16 hydrogen atoms within the 3×2 supercell.

To find the stable atomic structures of CNT(3,3) on the patterned hydrogen-terminated Si(001) surfaces, the CNT(3,3) is initially placed on top of the dangling bonds of the surface by aligning the tube axis in parallel with the surface dangling-bond rows. To describe all the initial configurations of the CNT(3,3) on the surface, a configuration of the CNT corresponding to zero rotation should be defined. The zero-degree rotational configuration is the one where one of the C-C-dimer rows along the tube axis is lying closest to the Si surface. The zero-degree rotational configuration

of CNT(3,3) on the pattern-1 surface is shown in Fig. 2 and an identical orientation of the tube corresponds to the zero-degree rotational configuration of the CNT(3,3) on Si(001) surface with pattern 2 and pattern 3. As the CNT(3,3) has a three-fold symmetry about the tube axis, various initial adsorption configurations are obtained by giving 40° , 80° , and 100° counterclockwise rotations to the tube about the tube axis with respect to the zero-degree rotational configuration. These initial adsorption configurations of the CNT(3,3) on patterned hydrogen-terminated Si(001) surfaces are denoted as Pattern- $N(\theta)$, where N represents the surface-pattern index, 1, 2, or 3, and θ represents the angle of rotation of the CNT(3,3) about its axis with respect to the zero-degree rotation. For example, Pattern-1(40) represents the initial configuration where the CNT(3,3) is placed on the hydrogen-terminated Si(001) surface having pattern 1 with a rotation of 40° to the CNT about its axis with respect to the zero-degree rotational configuration.

After having the relaxed structures of CNT(3,3) on a patterned hydrogen-terminated Si surface, an important quantity, the work function, is calculated by taking the difference between the vacuum-level energy (Φ) and the Fermi-level energy (E_f):

$$\text{WF} = \Phi - E_f. \quad (1)$$

The vacuum-level energy (Φ) is estimated by averaging the electrostatic potential [$V_{\text{av}}(z)$] on the X-Y plane at the center of the symmetrical slab along the Z axis (see Fig. 3).

Furthermore, the stark effect and hence the tuning of electrical properties including the work function of CNT(3,3) adsorbed on patterned hydrogen-terminated Si(001) surfaces is studied under the presence of an external electric field. To realize the external electric field, uniform charge sheets are placed in the vacuum on either side of the slab. Throughout our calculations the direction of the applied external electric field is perpendicular to the Si(001) surface and the positive (negative) electric field means that the surface is positively (negatively) biased. In this calculation, a variation of electric field (E) from -0.5 to 0.5 V/Å is considered. Note that in the presence of an external field,

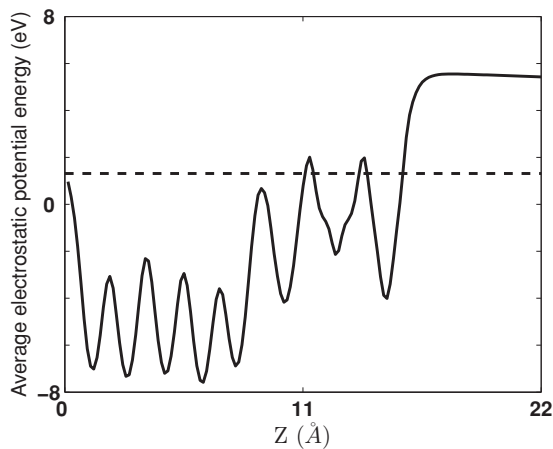


FIG. 3. The average electrostatic potential on the X-Y plane is plotted (solid line) along the Z axis for the Pattern-1(0) geometry. The Fermi level is shown by the dashed line.

the systems are allowed to undergo a complete atomistic relaxation.

III. RESULTS AND DISCUSSIONS

The results presented here include the energetics, the atomic structures, the band structures, the charge transfer, the work functions and the effect of external electric field on CNT(3,3) integrated on patterned hydrogen-terminated Si(001): 3×1 surfaces.

A. Structural and electrical properties

To find the most stable adsorption geometry of CNT(3,3) on the patterned hydrogen-terminated Si(001): 3×1 surfaces, binding energies per unit length (BE) of a CNT(3,3) supported by the patterned hydrogen-terminated Si(001): 3×1 surfaces having pattern 1 to pattern 3 are calculated. The BE of CNT(3,3) is defined as

$$\text{BE} = \frac{E_{\text{tot}}[\text{CNT} + \text{Si}] - E_{\text{tot}}[\text{Si}] - E_{\text{tot}}[\text{CNT}]}{L}, \quad (2)$$

where $E_{\text{tot}}[\text{CNT} + \text{Si}]$ is the total energy of the integrated system [i.e., CNT(3,3) supported by the patterned hydrogen-terminated Si(001): 3×1 surface] within the 3×2 supercell, $E_{\text{tot}}[\text{Si}]$ is the total energy of the patterned hydrogen-terminated Si(001): 3×1 surface within the 3×2 supercell, $E_{\text{tot}}[\text{CNT}]$ is the total energy of the CNT(3,3) within the 3×2 supercell, and L is the length of the CNT(3,3) cell within the 3×2 supercell.

The BEs for the CNT(3,3) on the hydrogen-terminated Si(001): 3×1 surface with pattern 1, pattern 2, and pattern 3 are displayed in Table I for $\theta = 0^\circ$, 40° , 80° , and 100° , respectively. It is clear from the Table I that the BE of CNT(3,3) on the hydrogen-terminated Si(001): 3×1 surface having pattern 1 is 0.546 eV/Å and it is independent of the initial (starting) configuration of the CNT(3,3) on the surface. An analysis of the relaxed atomic structures reveals

TABLE I. After complete relaxation, the binding energy per unit length (BE), the C-Si bond length, and the height of CNT from the Si surface, corresponding to different initial configurations of CNT(3,3) on patterned hydrogen-terminated Si(001): 3×1 surfaces are tabulated.

Initial configuration of CNT	BE (eV/Å)	d(C-Si) (Å)	Height (Å)
Pattern-1(0)	0.546	1.68–1.96	≈ 1.41
Pattern-1(40)	0.546	1.68–1.96	≈ 1.41
Pattern-1(80)	0.546	1.68–1.96	≈ 1.41
Pattern-1(100)	0.546	1.68–1.96	≈ 1.41
Pattern-2(0)	0.261	2.03–2.78	≈ 1.71
Pattern-2(40)	0.262	2.03–2.78	≈ 1.71
Pattern-2(80)	0.249	2.00–2.06	≈ 1.95
Pattern-2(100)	0.262	2.03–2.78	≈ 1.71
Pattern-3(0)	0.342	1.89–1.91	≈ 1.37
Pattern-3(40)	0.342	1.89–1.91	≈ 1.37
Pattern-3(80)	0.335	1.93–1.95	≈ 1.75
Pattern-3(100)	0.343	1.89–1.91	≈ 1.37

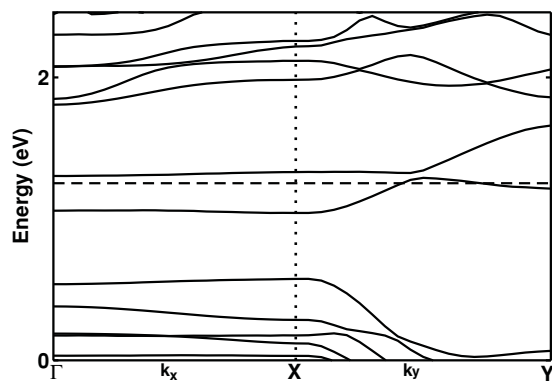


FIG. 4. The band structure of CNT(3,3) integrated on the hydrogen-terminated Si(001): 3×1 surface having pattern 1. The dashed line indicates the Fermi-level energy.

that all the initial configurations of the CNT(3,3) converge to a single geometry on the surface having pattern 1. The value of BE implies a strong interaction of the CNT(3,3) with the patterned hydrogen-terminated Si(001): 3×1 surface. To understand the electrical nature of the CNT(3,3) integrated on the hydrogen-terminated Si(001): 3×1 surface with pattern 1, the band structure is plotted in Fig. 4 and it shows that a single band crosses the Fermi level along the direction of the tube axis.

Therefore, we conclude that the CNT(3,3) integrated on the hydrogen-terminated Si(001): 3×1 surface having pattern 1 is metallic in nature. The optimized (fully relaxed) atomic structure of the CNT(3,3) supported by the hydrogen-terminated Si(001): 3×1 surface having pattern 1 is shown in Fig. 5. After complete optimization, the surface Si dimers buckle with a buckling angle of 5.07° from its original orientation and the length of each Si dimer changes from 2.42 to 2.49 Å, which gives an indication of strong interaction between CNT(3,3) and the hydrogen-terminated Si(001): 3×1 surface having pattern 1. The distribution of the C-Si bond lengths ranges within 1.68 to 1.96 Å. The nanotube resides approximately 1.41 Å above the surface. In the surface contact region, the C-C bond lengths are in the range of 1.39–1.69 Å.

In the case of integration of CNT(3,3) on the hydrogen-terminated Si(001): 3×1 surface having pattern 2, the initial configurations [Pattern-2(θ) with $\theta = 0^\circ, 40^\circ$, and 80°] converge to a more stable atomic structure with BE = 0.262 eV/Å. The configuration Pattern-2(80) converges to a less stable geometry with BE = 0.249 eV/Å. For the most stable geometry of the CNT(3,3) on the hydrogen-terminated Si(001): 3×1 surface having pattern 2, the C-Si bond lengths range from 2.03 to 2.78 Å and the height of the nanotube from the surface is ≈ 1.71 Å. The atomic structure for the most stable configuration of CNT(3,3) supported by the hydrogen-terminated Si(001): 3×1 surface having pattern 2 is shown in Fig. 6. We notice that in spite of the interaction of the CNT(3,3) with the surface, the tubular structure of the CNT(3,3) remains almost preserved.

The band structure for the most stable configuration of CNT(3,3) supported by the hydrogen-terminated Si(001): 3×1 surface having pattern 2 is shown in Fig. 7. The band-structure plot clearly shows that a band crosses the Fermi

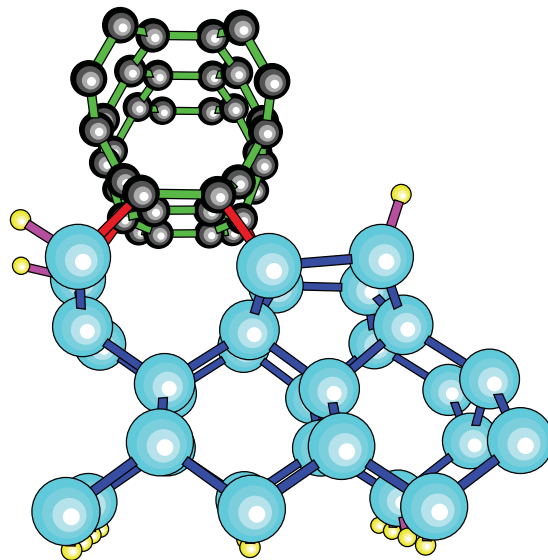


FIG. 5. (Color online) The optimized atomic structure of the most favorable geometry of the CNT(3,3) integrated on the hydrogen-terminated Si(001): 3×1 surface having pattern 1 [i.e., Pattern-1(0)].

level and thus the CNT(3,3) integrated on the patterned hydrogen-terminated Si(001): 3×1 surface having pattern 2 becomes metallic in nature.

The results for the adsorption of CNT(3,3) on the hydrogen-terminated Si(001): 3×1 surface having pattern 3 clearly shows that the initial configurations, Pattern-3(θ) with $\theta = 0^\circ, 40^\circ$, and 80° converges to a single geometry (most stable) with BE = 0.342 eV/Å. The initial configuration Pattern-3(80) leads to the least stable configuration with BE = 0.335 eV/Å. The C-Si bond lengths in the surface contact region range from 1.89–1.91 Å and the height of the nanotube from the surface is approximately 1.37 Å. The band-structure (see Fig. 8) analysis is done for the most favorable configuration, it is found that

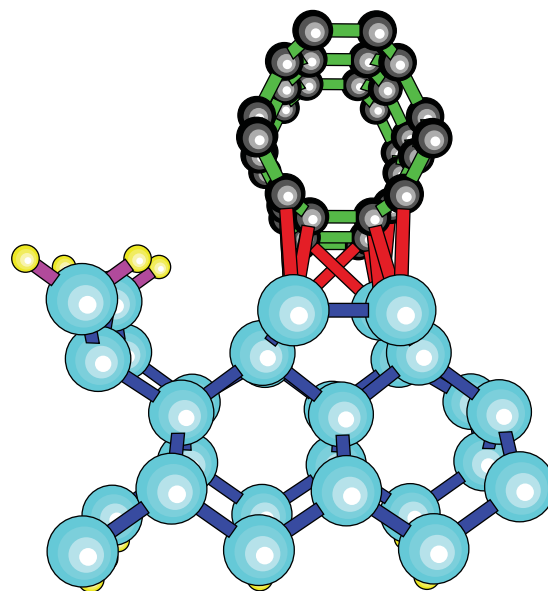


FIG. 6. (Color online) The optimized atomic structure of the most favorable geometry of the CNT(3,3) integrated on the hydrogen-terminated Si(001): 3×1 surface having pattern 2 [i.e., Pattern-2(0)].

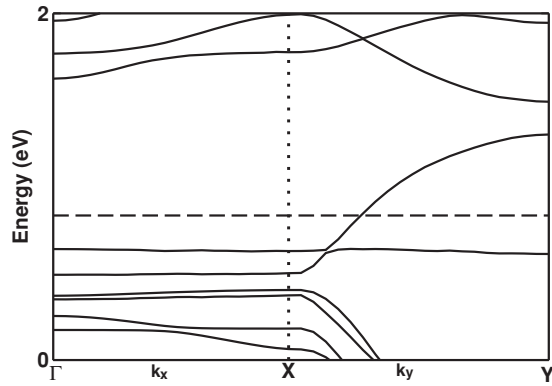


FIG. 7. Band structure of the most favorable geometry of the CNT(3,3) integrated on the hydrogen-terminated Si(001):3 × 1 surface having pattern 2. The Fermi-level energy is shown by the dashed line.

the CNT(3,3) supported by the hydrogen-terminated Si(001) surface having pattern 3 becomes nonmetallic in nature with a band gap ≈ 0.17 eV.

Comparing the BEs of the adsorbed CNT(3,3) on the hydrogen-terminated Si(001):3 × 1 surface having pattern 1, pattern 2, and pattern 3 we find that the relaxed structure on the hydrogen-terminated Si(001):3 × 1 surface having pattern 1 with BE = 0.546 eV/Å (see Fig. 5) is energetically most favorable. But earlier studies found that the most stable geometry of CNT(3,3) supported by a clean Si(001):2 × 1 surface¹² was nonmetallic in nature. One of the important results in this study is that depending on the choice of the patterned hydrogen-terminated Si(001) substrate one may obtain CNT(3,3) integrated on the Si(001) substrate with metallic or semiconducting character.

To estimate the degree of deformation of CNT(3,3) on the hydrogen-terminated Si(001):3 × 1 surface, we calculate the deformation ratio, which is defined as

$$\Delta R = \frac{(R_{\max} - R_{\min})}{R}, \quad (3)$$

where R_{\max} and R_{\min} are the maximum and minimum radii of the CNT(3,3) after the complete optimization on the patterned hydrogen-terminated Si(001):3 × 1 surface, and R

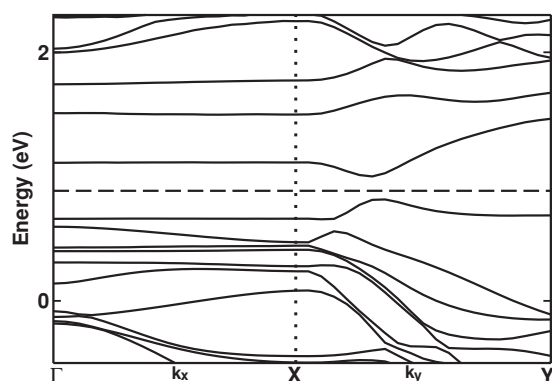


FIG. 8. The band structure of CNT(3,3) on the hydrogen-terminated Si(001):3 × 1 surface having pattern 3 [i.e., Pattern-3(0)]. The dashed line indicates the Fermi-level energy.

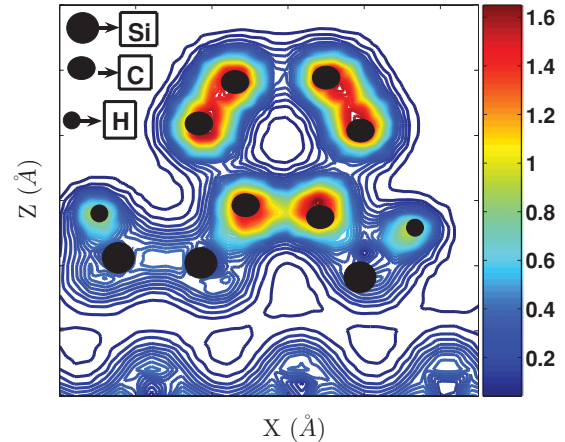


FIG. 9. (Color online) Total-charge-density plot on the X-Z plane for the most stable geometry of CNT(3,3) integrated on the hydrogen-terminated Si(001):3 × 1 surface.

is the average radius of the relaxed CNT(3,3). For the most stable geometry of the CNT(3,3) on the hydrogen-terminated Si(001):3 × 1 surface (shown in Fig. 5), the deformation ratio is 7.25%, which is smaller than the deformation ratio (of 26%) when the CNT(3,3) interacts with the clean Si(001):2 × 1 surface.¹² The smaller deformation of CNT(3,3) is clear from the total-charge-density plot on the X-Z plane of the most stable geometry of the CNT(3,3) integrated on the hydrogen-terminated Si(001):3 × 1 surface (see Fig. 9). This clearly indicates that the CNT(3,3) is less interactive with the patterned hydrogen-terminated Si(001) surface than with the clean Si(001):2 × 1 surface. This is reasonable because the dangling bonds of the adjacent Si-atoms row are passivated by hydrogen atoms.

To understand the direction of charge transfer in the most stable configuration of CNT(3,3) on hydrogen-terminated Si(001):3 × 1 surface, we have performed charge redistribution analysis. This is done by calculating the total-charge-density difference, $\Delta\rho$, which is obtained by subtracting the total charge density of the isolated CNT(3,3) ($\rho[\text{CNT}]$) and that of the isolated hydrogen-terminated Si(001):3 × 1 surface ($\rho[\text{Si}]$) from the total charge density of CNT(3,3) supported on the Si(001):3 × 1 surface ($\rho[\text{CNT} + \text{Si}]$):

$$\Delta\rho = \rho[\text{CNT} + \text{Si}] - \rho[\text{Si}] - \rho[\text{CNT}] \quad (4)$$

The total-charge-density difference ($\Delta\rho$) in the X-Z plane and that along the line of a Si-C bond for the most stable geometry of CNT(3,3) on the patterned hydrogen-terminated Si(001):3 × 1 surface are shown in Figs. 10 and 11, respectively. Figures 10 and 11 clearly show that charge transfer has taken place from the hydrogen-terminated Si(001):3 × 1 surface to CNT(3,3) and some charge is accumulated throughout the nanotube and the surface contact region. Bader charge analysis^{38,39} reveals that within the 3 × 2 supercell, a net amount of charge of 2.22e is transferred from the surface to the carbon nanotube. This is reasonable because the carbon atoms in the nanotube are more electronegative compared to the hydrogen and silicon atoms in the substrate. We also carried out Bader analysis to estimate the charge transfer in the patterned hydrogen-terminated Si(001):3 × 1 surface with

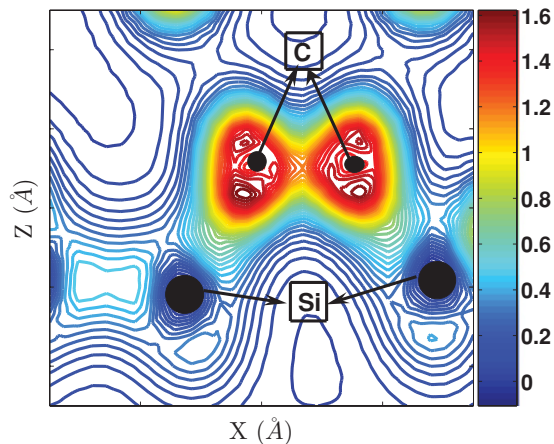


FIG. 10. (Color online) Charge-density-difference plot on the X-Z plane between C and Si atom of the most stable geometry of CNT(3,3) integrated on the hydrogen-terminated Si(001):3 \times 1 surface.

pattern 1 and it is found that some amount of charge transfers to each hydrogen atom from the Si(001) surface. This is also rational because hydrogen atoms are more electronegative compared to Si atoms.

B. Work function

The work function is an important quantity for a material that helps in understanding Schottky barrier height (SBH) and also helps in designing electrical devices. Therefore, to have a clear picture of the work functions of the systems, we have estimated the work functions of a clean Si(001):2 \times 1 surface, a clean Si(001):3 \times 1 surface, hydrogen-terminated Si(001):3 \times 1 surfaces with various patterns, an isolated CNT(3,3), and systems where CNT(3,3) is integrated on the patterned hydrogen-terminated Si(001):3 \times 1 surfaces (see Table II).

From Table II we see that the work function of the clean Si(001):2 \times 1 surface is 4.90 eV while that of the clean Si(001):3 \times 1 surface is 4.97 eV. This is rational because the hydrogen-terminated Si(001):3 \times 1 surface has more dangling bonds causing the presence of stronger surface dipoles pointing into the plane of the surface. We also notice that the work functions of the fully hydrogen-terminated

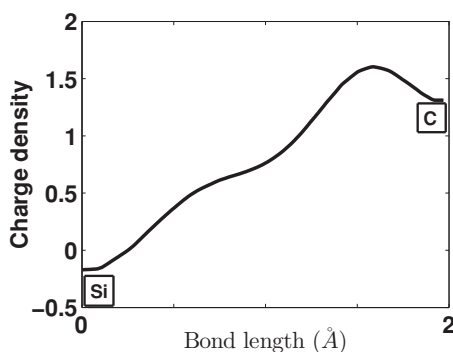


FIG. 11. Charge-density-difference plot along a C-Si bond of the most stable geometry of CNT(3,3) integrated on the hydrogen-terminated Si(001):3 \times 1 surface.

TABLE II. The work functions of CNT(3,3) patterned hydrogen-terminated Si(001):3 \times 1 surfaces and that of the CNT(3,3) integrated on patterned hydrogen-terminated Si(001):3 \times 1 surface.

System	Work function (eV)
CNT(3,3)	4.35
Clean Si(001):2 \times 1 surface	4.90
Si(001):3 \times 1 surface in which the bottom layer of Si atoms is passivated by H atoms	4.97
Si(001):3 \times 1 surface in which the bottom and upper layers of Si atoms are passivated by H atoms	4.76
Hydrogen-terminated Si(001):3 \times 1 surface having pattern 1	4.80
Hydrogen-terminated Si(001):3 \times 1 surface having pattern 2	4.80
Hydrogen-terminated Si(001):3 \times 1 surface having pattern 3	4.77
Pattern-1(0)	4.27
Pattern-1(40)	4.27
Pattern-1(80)	3.89
Pattern-1(100)	4.27
Pattern-2(0)	4.15
Pattern-2(40)	4.15
Pattern-2(80)	4.15
Pattern-2(100)	4.15
Pattern-3(0)	4.61
Pattern-3(40)	4.61
Pattern-3(80)	4.52
Pattern-3(100)	4.61

Si(001):3 \times 1 surfaces (4.76 eV) is smaller than that of a clean Si(001):3 \times 1 surface. The work functions of hydrogen-terminated Si(001):3 \times 1 surfaces with pattern 1, pattern 2, and pattern 3 are 4.80, 4.80, and 4.77 eV, respectively. Thus, we find that the work function of the hydrogen-terminated Si(001):3 \times 1 surface decreases with the increase of hydrogen coverage. This trend of variation of work function with hydrogen coverage on Si(001) surface agrees with an experimental observation.⁴⁰ Note that the work function of the Si(001):3 \times 1 surface decreases due to hydrogen adsorption in spite of having a charge transfer from the Si(001) surface to adsorbed hydrogen atoms. This is because, apart from the dependence of the work function on the charge transfer from the substrate (Si surface) to adsorbate (hydrogen atoms), it also depends on the hybridization between the adsorbate and substrate and the relaxation of the substrate induced by the adsorbate.^{40,41}

The work function of the isolated CNT(3,3) is found to be 4.35 eV, which is lower than those of the hydrogen-terminated Si(001):3 \times 1 surfaces. When the CNT(3,3) is adsorbed on the hydrogen-terminated Si(001):3 \times 1 surface with pattern 1, the work function for the most favorable configuration turns out to be 4.27 eV, which is less than that of the substrates. We have already noted that in this case, charge transfer takes place from the substrate to CNT(3,3) and therefore the decrease of work function due to adsorption of CNT(3,3)

on the Si(001):3 × 1 surface with pattern 1 may appear to be unconventional [as in the case of hydrogen adsorption on Si(001) surface]. However, the decrease of work function due to adsorption of CNT(3,3) on the Si(001):3 × 1 surface with pattern 1 is possible because the variation of work function not only depends on the charge transfer due to electronegativity, it also depends on the hybridization between the adsorbate and substrate and the relaxation of the substrate induced by the adsorbate.

For completeness we have also found the work function of the CNT(3,3) integrated Si(001):3 × 1 surfaces with other configurations. For example, the work function of the least favorable configuration of CNT(3,3) on the Si(001):3 × 1 surface with pattern 1 is 3.89 eV; the work function of CNT(3,3) when supported on the hydrogen-terminated Si(001):3 × 1 surface with pattern 2 is 4.15 eV. Finally, when the CNT(3,3) is supported on the hydrogen-terminated Si(001):3 × 1 surface with pattern 3, the work function for the most favorable configuration is 4.61 eV and that for the least favorable configuration is 4.52 eV.

C. Effect of the external electric field of CNT(3,3) integrated on a hydrogen-terminated Si(001):3 × 1 surface.

Here, our objective is to understand the influence of electric field (E) on the energetics and electrical properties (including work function) of the most stable CNT(3,3) integrated on hydrogen-terminated Si(001):3 × 1 surface having pattern 1. The adsorption energy per unit length (BE_{EF}) of the CNT(3,3) supported on hydrogen-terminated Si(001):3 × 1 surface in the presence of an external electric field is defined as

$$BE_{EF} = \frac{E_{tot}[CNT + Si]_{EF} - E_{tot}[Si]_{EF} - E_{tot}[CNT]_{EF}}{L}, \quad (5)$$

where $E_{tot}[CNT + Si]_{EF}$, $E_{tot}[Si]_{EF}$, and $E_{tot}[CNT]_{EF}$ are the total energy of the composite system, the isolated hydrogen-terminated Si(001):3 × 1 surface, and the isolated CNT(3,3), respectively, in the presence of an external electric field. The

TABLE III. For various electric-field strengths along the z direction, the adsorption energies of CNT(3,3) integrated on the hydrogen-terminated Si(001):3 × 1 surface having pattern 1 with reference to those in the absence of electric field (ΔE) and the work function of the system in the respective electric field are tabulated.

Pattern	Electric field (V/Å)	ΔE (eV)	Work function (eV)
pattern 1	-0.5	-0.599	4.23
pattern 1	-0.4	-0.502	4.24
pattern 1	-0.3	-0.299	4.24
pattern 1	-0.2	-0.074	4.27
pattern 1	-0.1	-0.027	4.27
pattern 1	0.0	0.000	4.27
pattern 1	0.1	-0.041	4.27
pattern 1	0.2	0.003	4.27
pattern 1	0.3	-0.293	4.28
pattern 1	0.4	-0.502	4.29
pattern 1	0.5	-0.764	4.29

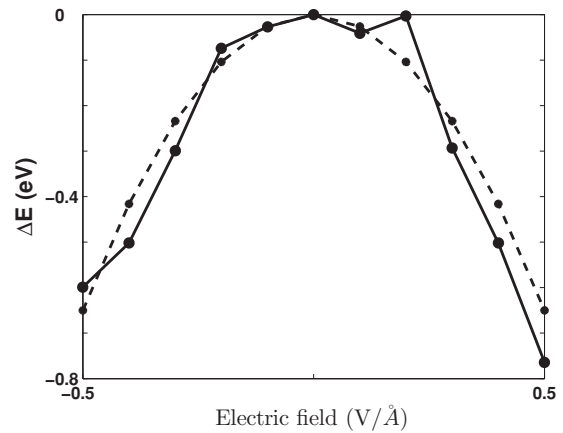


FIG. 12. Variation of the relative adsorption energy (the adsorption energy in the presence of an external electric field with respect to the zero-field adsorption energy) of the most stable geometry of CNT(3,3) integrated on patterned hydrogen-terminated Si(001):3 × 1 surface is shown by the solid curve. The variation is fitted by the dotted curve, $\Delta E = -2.6E^2$.

adsorption energy in the presence of an electric field increases with increasing field strength. For various field strengths, the adsorption energies of the CNT(3,3) integrated on a hydrogen-terminated Si(001):3 × 1 surface in the presence of an external electric field with reference to the adsorption energy in the absence of the field (ΔE) are calculated and they are presented in Table III. The variation of relative adsorption energies (ΔE) with the applied electric field is given in Fig. 12 and it shows a parabolic nature: $\Delta E = -2.6 E^2$. This parabolic nature is expected because the dipoles created due to the electric field are created in proportion to the electric field and consequently, the energy associated with these dipoles is proportional to the square of electric field (i.e., an electric-polarization effect).

To understand the variation of the work function due to the external electric field (E), we have also calculated the work function of the most stable CNT(3,3) supported on a hydrogen-terminated Si(001):3 × 1 surface in the presence of an electric field and the results are given in Table III. Our results

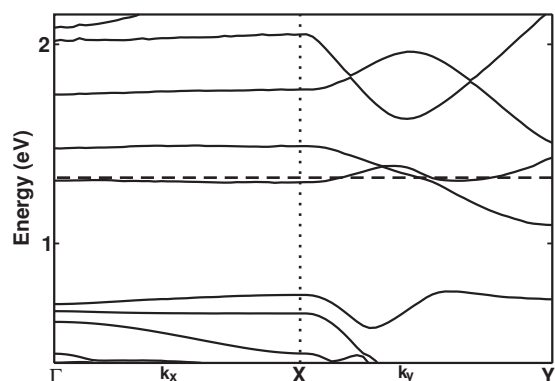


FIG. 13. Band structure of the most stable geometry of CNT(3,3) integrated on a hydrogen-terminated Si(001):3 × 1 surface in the presence of an external electric field of -0.5 V/Å . The dashed line indicates the Fermi-energy level.

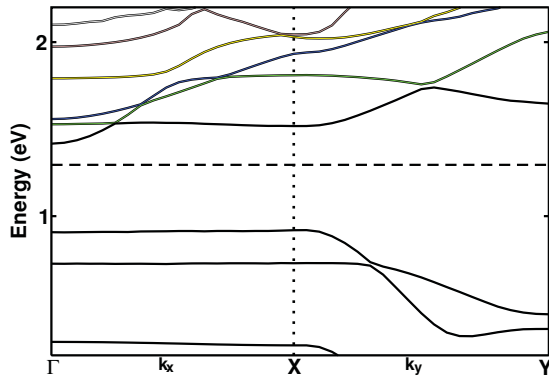


FIG. 14. (Color online) Band structure of the most stable geometry of CNT(3,3) integrated on a hydrogen-terminated Si(001):3 × 1 surface in the presence of an external electric field of 0.5 V/Å. The Fermi-level energy is indicated by dashed line.

clearly show that the work function increases or decreases with the positive or negative electric field. The increase of work function due to the increase of electric-field strength along the z direction is understandable because the surface electrons are pulled into the surface by an electric force that is proportional to the electric field. In this calculation one of the significant results is that the hybrid structure, which was metallic in the absence of an electric field, becomes more metallic at $E = -0.5$ V/Å (see Fig. 13) and it becomes nonmetallic at $E = 0.5$ V/Å with a band gap ~ 0.6 eV (see Fig. 14). The variation of band gap of the most stable CNT(3,3) supported on hydrogen-terminated Si(001):3 × 1 surface with the external electric field is plotted in Fig. 15. We note a sudden opening of a band gap of ~ 0.48 eV at $E = 0.45$ V/Å. The band-gap opening in the presence of an external field may be due to a rearrangement of atoms of the system induced by the electric field. Thus, the electrical nature (metallicity and band gap) of the CNT(3,3) integrated on the patterned hydrogen-terminated Si(001):3 × 1 surface may be tuned by applying an external electric field. This phenomenon may open up an interesting avenue for application as switch devices and hence a new kind of CNT-based electronics.

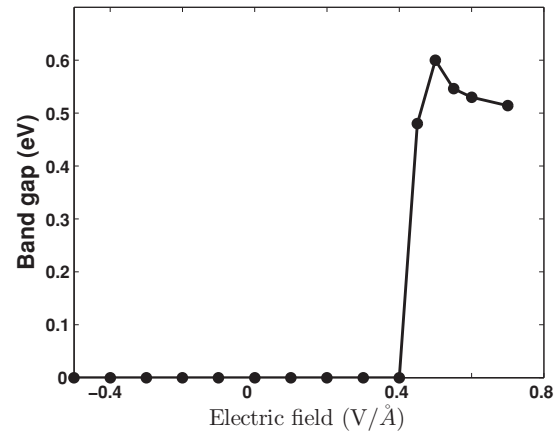


FIG. 15. Variation of the band gap with respect to the external electric field for the most stable geometry of CNT(3,3) integrated on a hydrogen-terminated Si(001):3 × 1 surface.

IV. SUMMARY

Among 4-Å diameter carbon nanotubes, the CNT(3,3) is chosen to integrate on patterned hydrogen-terminated Si(001):3 × 1 surfaces. Total-energy calculations are done under the density-functional formalism to find the most stable geometry of the CNT(3,3) on patterned hydrogen-terminated Si(001):3 × 1 surfaces. Our calculations reveal that the most stable hybrid structure is obtained when the CNT(3,3) is placed in between the dihydride- and monohydride-Si rows of the patterned hydrogen-terminated Si(001):3 × 1 surface. Band-structure analysis, work-function calculations, and charge-redistribution analysis are done for understanding the electrical properties of the integrated systems in detail. Furthermore, we have studied the effect of an external electric field on the electronic properties of the hybrid system and it is found that the most stable metallic hybrid structure turns into nonmetallic at $E = 0.45$ V/Å and becomes more metallic at $E = -0.5$ V/Å. Therefore, this study suggests that the CNT(3,3) integrated on the patterned hydrogen-terminated Si(001):3 × 1 surface may be used as a switching device under the action of an external electric field.

*bikashc.gupta@visva-bharati.ac.in

¹S. Iijima, *Nature (London)* **354**, 56 (1991); T. Ichihashi, *ibid.* **363**, 603 (1993).

²M. M. Treacy, T. W. Ebbesen, and J. M. Gibson, *Nature (London)* **381**, 678 (1996).

³J. P. Lu, *Phys. Rev. Lett.* **79**, 1297 (1997).

⁴E. Hernández, C. Goze, P. Bernier, and A. Rubio, *Phys. Rev. Lett.* **80**, 4502 (1998).

⁵R. Saito, G. Dresselhaus, and M. S. Dresselhaus, *Physical Properties of Carbon Nanotubes* (Imperial College Press, London, 2004).

⁶R. Saito, M. Fujita, G. Dresselhaus, and M. S. Dresselhaus, *Phys. Rev. B* **46**, 1804 (1992).

⁷R. Saito, M. Fujita, G. Dresselhaus, and M. S. Dresselhaus, *Appl. Phys. Lett.* **60**, 2204 (1992).

⁸R. Saito, G. Dresselhaus, and M. S. Dresselhaus, *J. Appl. Phys.* **73**, 494 (1993).

⁹W. Orellana, R. H. Miwa, and A. Fazzio, *Phys. Rev. Lett.* **91**, 166802 (2003).

¹⁰R. H. Miwa, W. Orellana, and A. Fazzio, *Appl. Phys. Lett.* **86**, 213111 (2005).

¹¹S. Berber and A. Oshiyama, *Phys. Rev. Lett.* **96**, 105505 (2006).

¹²G. W. Peng, A. C. H. Huan, L. Liu, and Y. P. Feng, *Phys. Rev. B* **74**, 235416 (2006).

¹³S. Barraza-Lopez, P. M. Albrecht, and J. W. Lydig, *Phys. Rev. B* **80**, 045415 (2009).

¹⁴S. Barraza-Lopez, P. M. Albrecht, N. A. Romero, and K. Hess, *J. Appl. Phys.* **100**, 124304 (2006).

¹⁵P. M. Albrecht, S. B. Lopez, and J. W. Lyding, *Nanotechnology* **18**, 095204 (2007).

¹⁶P. M. Albrecht and J. W. Lyding, *Appl. Phys. Lett.* **83**, 5029 (2003).

¹⁷K. Kamaras, M. E. Itkis, H. Hu, B. Zhao, and R. C. Haddon, *Science* **301**, 1501 (2003).

- ¹⁸P. M. Albrecht and J. W. Lyding, *Nanotechnology* **18**, 125302 (2007).
- ¹⁹L. B. Ruppalt and J. W. Lyding, *Nanotechnology* **18**, 215202 (2007).
- ²⁰P. M. Albrecht, S. B. Lopaz, and J. W. Lyding, *Small* **3**, 1402 (2007).
- ²¹J. J. Boland, *Adv. Phys.* **42**, 129 (1993).
- ²²F. S. Tautz and J. A. Schaefer, *J. Appl. Phys.* **84**, 6636 (1998).
- ²³Y. J. Chabal and K. Raghavachari, *Phys. Rev. Lett.* **54**, 1055 (1985).
- ²⁴J. J. Boland, *Phys. Rev. Lett.* **65**, 3325 (1990).
- ²⁵J. J. Boland, *Surf. Sci.* **261**, 17 (1992).
- ²⁶Y. J. Chabal and K. Raghavachari, *Phys. Rev. Lett.* **53**, 282 (1984).
- ²⁷T. C. Shen, C. Wang, G. C. Abein, J. R. Tucker, J. W. Lyding, Ph. Avouris, and R. E. Walkup, *Science* **268**, 1590 (1995).
- ²⁸J. N. Randall, J. W. Lyding, S. Schmucker, J. R. Von Ehr, J. Ballard, R. Saini, H. Xu, and Y. Ding, *J. Vac. Sci. Technol. B* **27**, 2764 (2009).
- ²⁹N. Wang, Z. K. Tang, G. D. Li, and J. S. Chen, *Nature (London)* **408**, 50 (2000).
- ³⁰G. Kresse and J. Hafner, *Phys. Rev. B* **47**, R558 (1993); **49**, 14251 (1994).
- ³¹G. Kresse and J. Furthmuller, *Phys. Rev. B* **54**, 11169 (1996).
- ³²G. Kresse and J. Furthmuller, *Comput. Mater. Sci.* **6**, 15 (1996).
- ³³G. Kresse and J. Hafner, *J. Phys. Condens. Matter B* **6**, 8245 (1994).
- ³⁴P. Sen, S. Ciraci, I. P. Batra, C. H. Grain, and S. Sivanathan, *Surf. Sci.* **519**, 79 (2002).
- ³⁵C. Hobbs, L. Kantorovich, and J. D. Gale, *Surf. Sci.* **591**, 45 (2005).
- ³⁶M. W. Radny, P. V. Smith, T. C. G. Rrusch, O. Warschkow, N. A. Marks, H. F. Wilson, S. R. Schofield, N. J. Curson, D. R. McKenzie, and M. Y. Simmons, *Phys. Rev. B* **76**, 155302 (2007).
- ³⁷M. Ceriotti and M. Bernasconi, *Phys. Rev. B* **76**, 245309 (2007).
- ³⁸R. Bader, *Atoms in Molecules: A Quantum Theory* (Oxford University Press, New York, 1990).
- ³⁹W. Tang, E. Sanville, and G. Henkelman, *J. Phys.: Condens. Matter* **21**, 084204, (2009).
- ⁴⁰D.-S. Lin, T. Miller, T.-C. Chiang, R. Tsu, and J. E. Greene, *Phys. Rev. B* **48**, 11846 (1993).
- ⁴¹T. C. Leung, C. L. Kao, W. S. Su, Y. J. Feng, and C. T. Chan, *Phys. Rev. B* **68**, 195408 (2003).